Electronic Supplementary Material (ESI) for Journal of Materials Chemistry A.

Constructing robust gigantic drum-like hydrophobic [$Co_{24}U_6$] nanocage in metal-organic framework for high-performance SO_2 removal at humidity condition

Yaling Fan,[a] Mengjia Yin,[a] Rajamani Krishna,[b] Xuefeng Feng,[a] and Feng Luo[a]*

[a]School of Chemistry, Biology and Materials Science, East China University of Technology, Nanchang 330013, P.R.China

*Corresponding Author(s): Feng Luo: ecitluofeng@163.com
[b]Van't Hoff Institute for Molecular Sciences, University of Amsterdam, Science Park 904, 1098 XH Amsterdam, The Netherlands

X-ray Crystallography. X-ray diffraction data of Cage-U-Co-MOF were collected at room temperature on a Bruker Appex II CCD diffractometer using graphite monochromated MoKα radiation (λ=0.71073 Å). The data reduction included a correction for Lorentz and polarization effects, with an applied multi-scan absorption correction (SADABS). The crystal structure was solved and refined using the SHELXTL program suite. Direct methods yielded all non-hydrogen atoms, which were refined with anisotropic thermal parameters. All hydrogen atom positions were calculated geometrically and were riding on their respective atoms. The SQUEEZE subroutine of the PLATON software[15] suite was used to remove the scattering from the highly disordered guest molecules. CCDC 2032794 contains the supplementary crystallographic data of Cage-U-Co-MOF. These data can be obtained free of charge from the Cambridge Crystallographic Data Centre via www.ccdc.cam.ac.uk/data_request/cif.

Fitting of experimental data on pure component isotherms

The isotherm data for SO_2 and CO_2 in Cage-U-Co-MOF at 298 K were fitted with the dual-site Langmuir model, where we distinguish two distinct adsorption sites A and B:

$$q = \frac{q_{sat,A} b_A p}{1 + b_A p} + \frac{q_{sat,B} b_B p}{1 + b_B p}$$

The unary isotherm fit parameters are provided in Table S2.

The isotherm data for N_2 in Cage-U-Co-MOF at 298 K was fitted with the 1-site Langmuir model

$$q = q_{sat} \frac{bp}{1 + bp}$$

The 1-site Langmuir fit parameters are provided in Table S3.

Isosteric heat of adsorption

The binding energy is reflected in the isosteric heat of adsorption, Q_{st}, is calculated from the Clausius-Clapeyron equation

$$Q_{st} = -RT^2 \left(\frac{\partial \ln p}{\partial T} \right)_q$$

For the 1-site Langmuir-Freundlich model the differentiation of the Clausius-Clapeyron equation can be carried out analytically.

IAST calculations of adsorption selectivities and uptake capacities

We consider the separation of binary mixtures at 298 K. The adsorption selectivity for SO_2/CO_2, SO_2/N_2 separation is defined by

$$S_{ads} = \frac{q_1/q_2}{p_1/p_2}$$

Transient breakthrough simulations

The performance of industrial fixed bed adsorbers is dictated by a combination of adsorption selectivity and uptake capacity. Transient breakthrough simulations were carried out using the methodology described in earlier publications (*Microporous Mesoporous Mater.* **2014**, *185*, 30-50; *Sep. Purif. Technol.* **2018**, *194*, 281-300; *ACS Omega* **2020**, *5*, 16987−17004). The following two mixtures were investigated.

1/99 SO_2/CO_2 mixtures at 298 K,

1/99 SO_2/N_2 mixtures at 298 K,

For the breakthrough simulations, the following parameter values were used: length of packed bed, L = 0.3 m; voidage of packed bed, ε = 0.4; superficial gas velocity at inlet, u = 0.04 m/s.

The *y*-axis is the dimensionless concentrations of each component at the exit of the fixed bed, c_i/c_{i0} normalized with respect to the inlet feed concentrations. The *x*-axis is the *dimensionless* time, $\tau = \frac{tu}{L\varepsilon}$, defined by dividing the actual time, *t*, by the characteristic time, $\frac{L\varepsilon}{u}$.

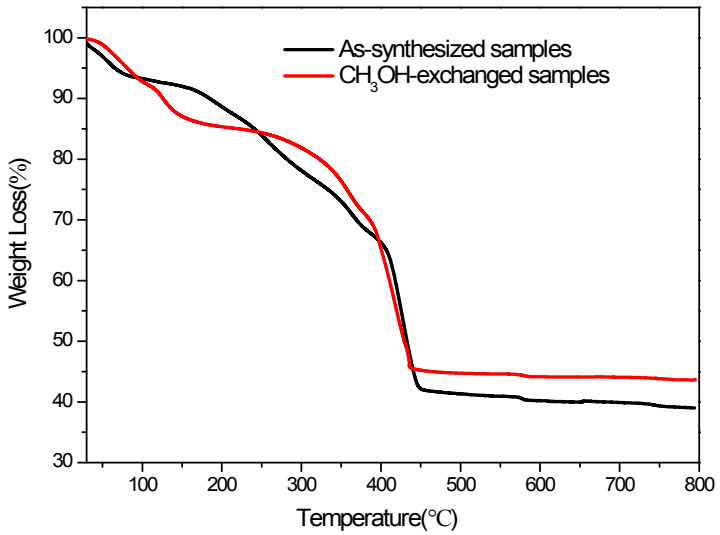

Fig. S1 The TG plot of **Cage-U-Co-MOF** and the CH_3OH-exchanged samples.

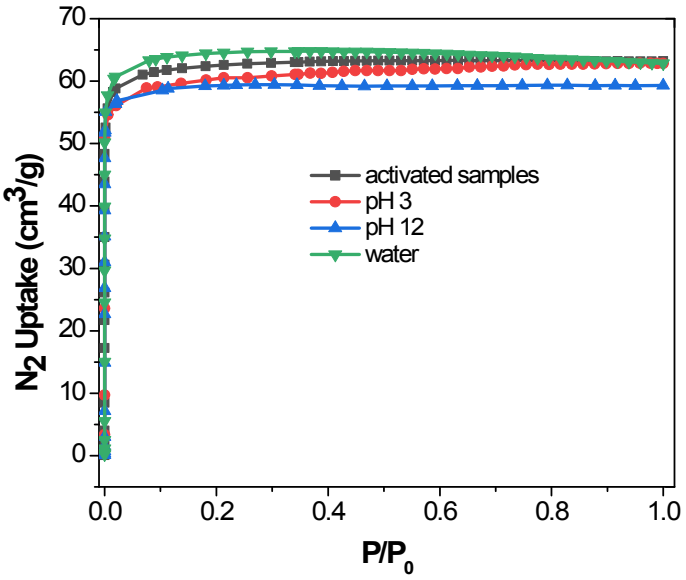

Fig. S2 A comparison of Ar adsorption at 77 K for the activated samples and the samples after immersing in water and pH=3 and 12 solution. The corresponding BET surface area is 208 m^2/g, 212m^2/g, 201 m^2/g, and 199 m^2/g, respectively.

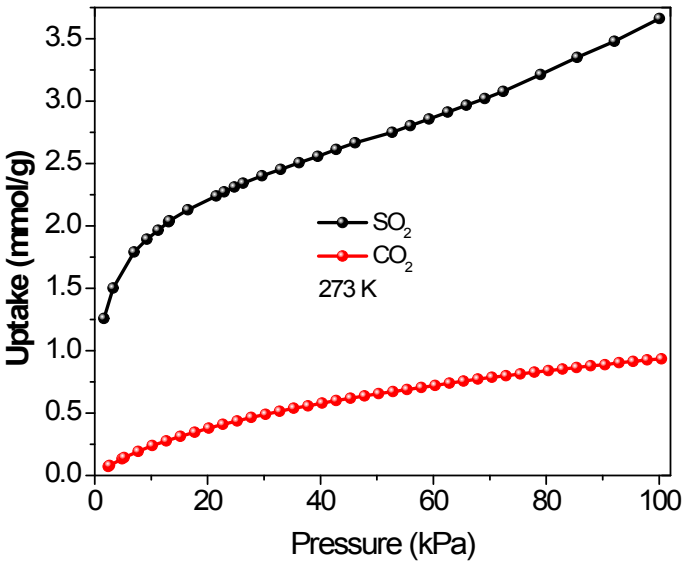

Fig. S3 The SO_2 and CO_2 adsorption at 273 K.

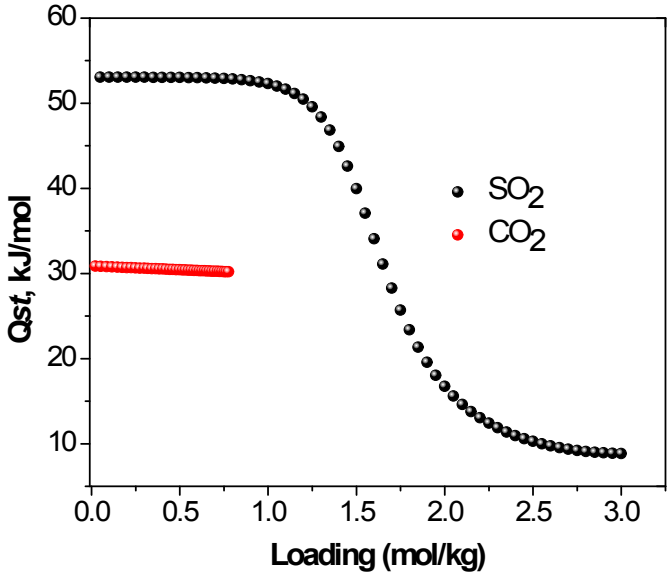

Fig. S4 The Qst value of SO_2 and CO_2 for **Cage-U-Co-MOF**.

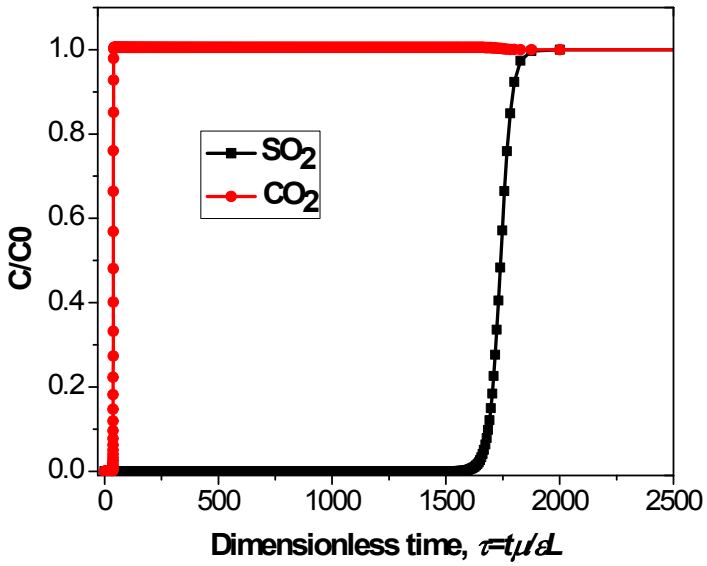

Fig. S5 The transient breakthrough simulations for a 1:99 v/v SO_2/CO_2 mixture based on **Cage-U-Co-MOF** bed.

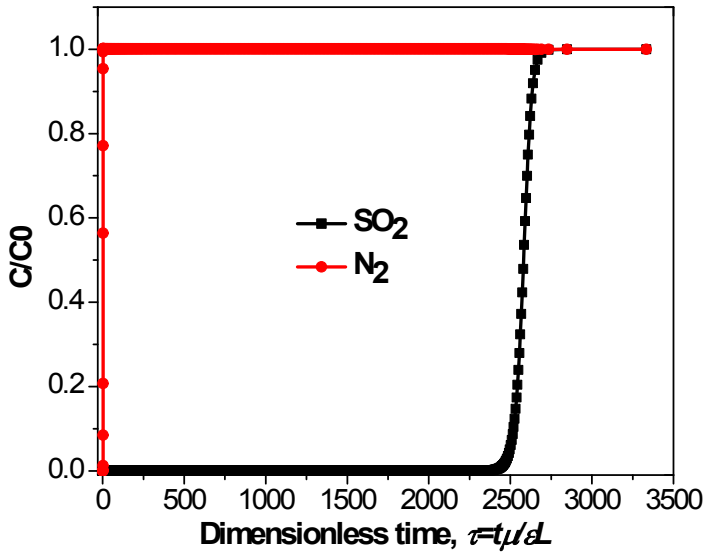

Fig. S6 The transient breakthrough simulations for a 1:99 v/v SO_2/N_2 mixture based on **Cage-U-Co-MOF** bed.

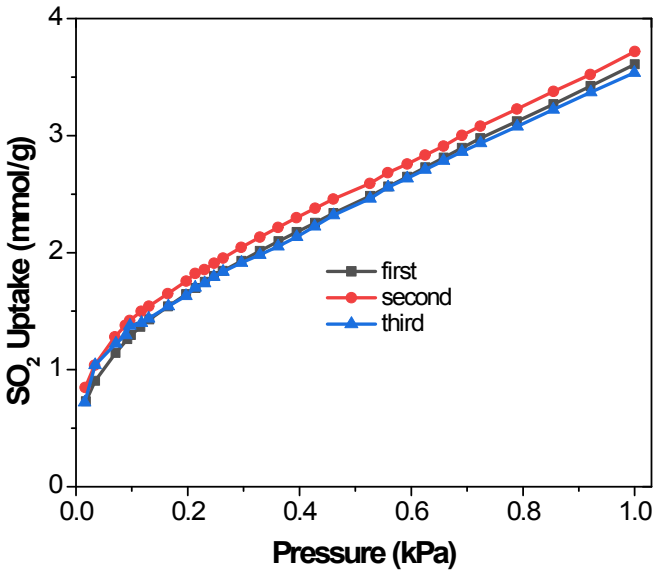

Fig. S7 Repeating SO_2 adsorption test for Cage-U-Co-MOF**.**

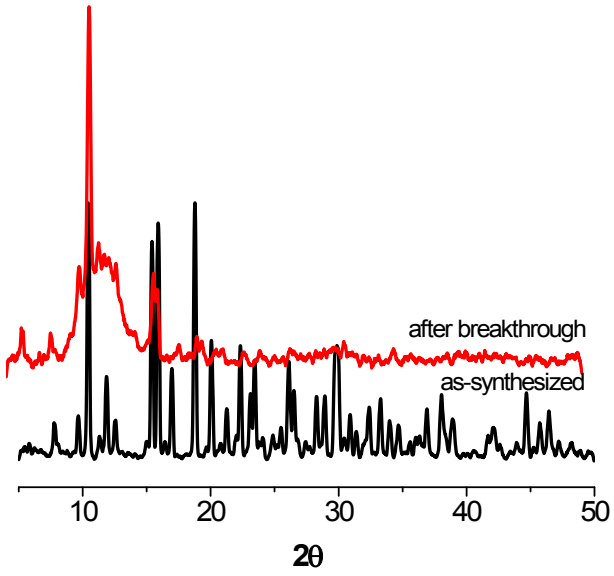

Fig. S8 A comparison of PXRD patterns of the as-synthesized samples and the samples after all breakthrough experiments.

Table S1. A comparison of reported MOFs for SO_2 removal.

MOF tpyes	SO_2 adsorption capacity (1 bar, 298 K), mmol/g	SO_2/CO_2 selectivity	References
SIFSIX-2-Cu-i	11.0	87.1	1
$Ni(bdc)(ted)_{0.5}$	9.97	-	2
MFM-300(In)	8.28	50	3
MFM-202a	10.2	-	4
NOTT-300 (Al)	7.1	-	5
MFM-170	17.5	28	6
MOF-5	Less than 0.016	-	7
IRMOF-3	0.094	-	7
MOF-74	3.03	-	7
MOF-199	0.5	-	7
P(TMGA-co-MBA)	4.0	-	8
Activated Carbon	3.3	-	9
Cage-U-Co-MOF	3.62	80.7	Our work

"-" denotes the data can not be obtaind from corresponding reference.

1.Cui. X. L.; Yang. Q. W.; Yang. L. F.; Krishna. R.; Zhang. Z. G.; Bao. Z. B.; Wu. H.; Ren. Q.; Zhou. W.; Chen. B. L.; Xing. H. B. Ultrahigh and selective SO_2 uptake in inorganic anion-pillared hybrid porous materials. *Advanced Materials*. **2017**. *29*.1606929(1-9).

2. Tan. K.; Canepa. P.; Gong. Q. H.; Liu. J.; Johnson. D. H.; Dyevoich. A.; Thallapally. P. K.; Thonhauser. T.; Li. J.; Chabal. Y. J. Mechanism of preferential adsorption of SO_2 into two microporous paddle wheel frameworks $M(bdc)(ted)_{(0.5)}$. *Chemistry of Materials*. **2013**. *25*. 4653-4662.

3. Savage. M.; Cheng .Y. Q.; Easun. T. L.; Eyley. J. E.; Argent.S. P.; Warren. M. R.; Lewis. W.; Murray. C.; Tang. C. C.; Frogley. M. D.; Cinque G.; Sun. J. L.; Rudic´. S.; Murden R. T.; Benham. M. J.; Fitch. A. N.; Blake. A. J.; Ramirez-Cuesta. A. J.; Yang. S. H.; Schroder. M. Selective Adsorption of Sulfur Dioxide in a Robust Metal–Organic Framework Material. *Advanced Materials*.

2016. *28*. 8705-8711.

4. Yang. S. H.; Liu. L. F.; Sun. J. L.; Thomas. K. M.; Davies A. J.; George. M. W.; Blake. A. J.; Hill. A. H.; Fitch. A. N.; Tang. C. C. , Chroeder. M. Irreversible network transformation in a dynamic porous host catalyzed by sulfur dioxide. *Journal of the American Chemical Society*. **2013**. *135*. 4954-4957.

5. Yang. S. H.; Sun. J. L.; Ramirez-Cuesta. A. J.; Callear. S. K.; David. W. F.; Anderson. D. P.; Newby. R.; Blake1. A. J.; Parker. J. E.; Tang. C. C.; Schro¨der1. M. Selectivity and direct visualization of carbon dioxide and sulfur dioxide in a decorated porous host. *Nature chemistry.* **2012**. *4*.887-894.

6. Smith. G. L.; Eyley. J. E.; Han. X.; Zhang. X. R.; Li. J. N.; Jacques. N. M.; Godfrey. H. G. W.; Argent. S. P.; McPherson. L. J. M.; Teat. S. J.; Cheng Y. Q.; Frogley. M. D.; Cinque. G.; Day S. J.; C. C. Tang.; Easun . T. L.; Rudić. S.; Ramirez-Cuesta . A. J.; Yang. S.H.; Schro¨der1. M. Reversible coordinative binding and separation of sulfur dioxide in a robust metal–organic framework with open copper sites. *Nature Materials.* **2019**. *18*. 1358-1365.

7. Britt. D.; Tranchemontagne. D.; Yaghi O. M. Metal-organic frameworks with high capacity and selectivity for harmful gases. *Proceedings of the National Academy of Sciences of the United States of America*. **2008**. *105*. 11623-11627.

8. Wu. L. B.; An. D.; Dong. J.; Zhang. Z. M.; Li. B. G.; Zhu. S. P. Preparation and SO2 Absorption/Desorption Properties of Crosslinked Poly(1,1,3,3-Tetramethylguanidine Acrylate) Porous Particles. *Macromolecular Rapid Communications*. **2006**. *37*.1949-1954.

9. Yi. H. H.; Wang. Z. X.; Liu. H.Y.; Tang X. L.; Ma. D.; Zhao. S. Z.; Zhang. B. W.; Gao. F. Y.; Zuo Y. R. Adsorption of SO_2, NO, and CO_2 on Activated Carbons: Equilibrium and Thermodynamics . *Journal of Chemical & Engineering Data.* **2014**. *59*. 1556-1563.

Table S2. Dual-site Langmuir parameter fits for SO_2 and CO_2 in Cage-U-Co-MOF at 298 K.

	Site A		Site B	
	$q_{A,sat}$ mol kg^{-1}	b_A Pa^{-1}	$q_{B,sat}$ mol kg^{-1}	b_B Pa^{-1}
SO_2	11	2.875E-06	1.1	8.548E-04

CO_2	0.2	5.562E-06	2	5.441E-06

Table S3. 1-site Langmuir parameter fits for N_2 in Cage-U-Co-MOF at 298 K.

	q_{sat} mol kg^{-1}	b Pa^{-1}
N_2	0.15	3.21095E-06